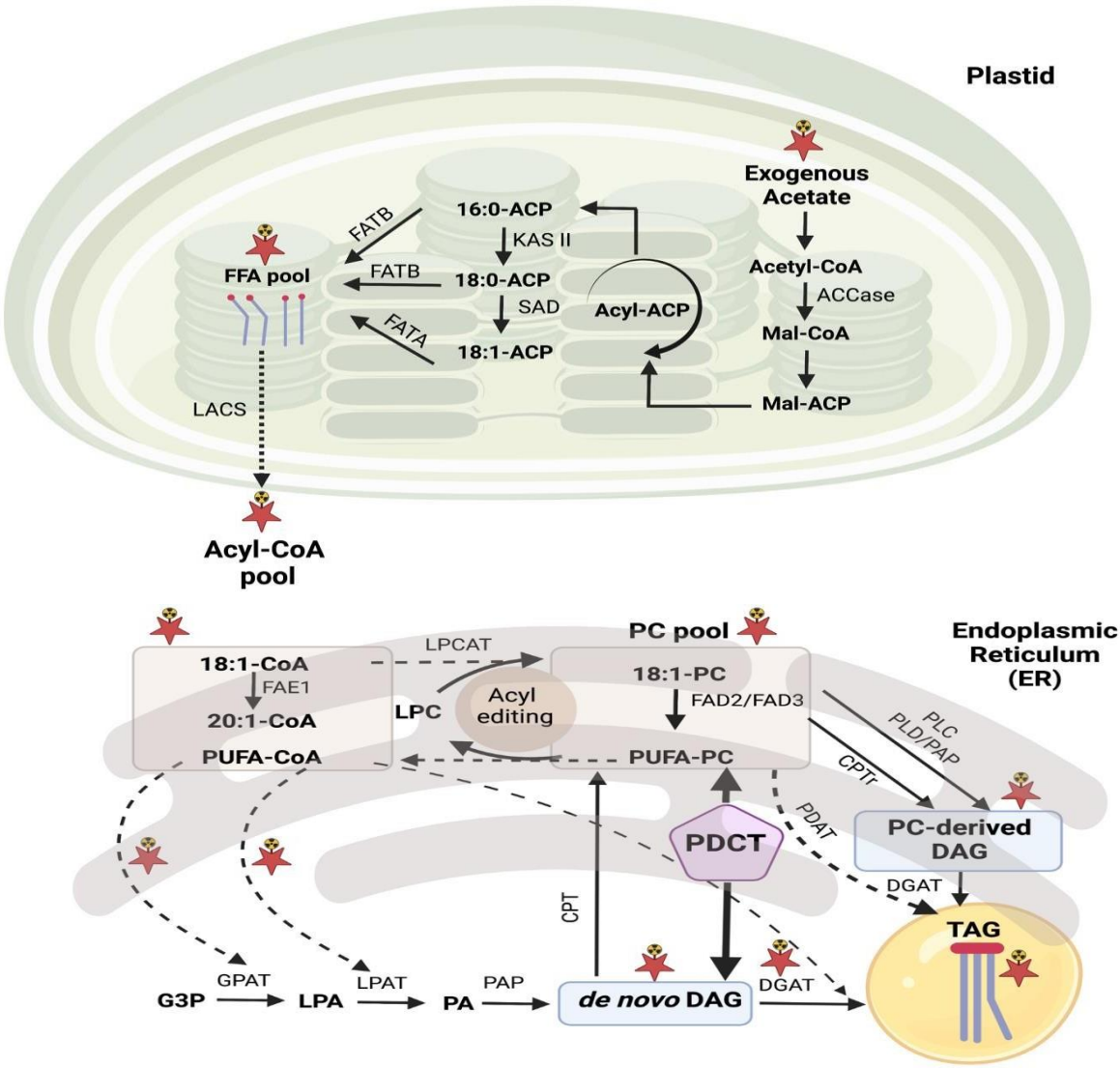

Figure. 1 A simplified metabolic network of seed TAG synthesis incorporating PDCT enzyme. The possible routes for acyl chain incorporation into TAG in oilseeds are shown. The red stars indicate possible labeling to enzymatic reactions with [14C] incorporated from exogenous acetate. Solid lines: flux through glycerol backbone. Dashed lines: acyl fluxes. Abbreviations-lipids: PDCT, phosphatidylcholine:diacylglycerol cholinephosphotransferase; DAG, diacylglycerol; TAG, triacylglycerol; G3P, glycerol-3- phosphate; LPA, lysophosphatidic acid; LPC, lysophosphatidylcholine; PA, phosphatidic acid; PC, phosphatidylcholine; PUFA, polyunsaturated fatty acids; FFA, free fatty acids; Mal-ACP, Malonyl-[acyl-carrier protein]. Abbreviations-enzymatic or transport reactions: ACCase, acetyl-CoA carboxylase; CPT, CDP-choline:diacylglycerol cholinephosphotransferase; CPTr, CPT reverse; DGAT, acyl-CoA:diacylglycerol acyltransferase; Acyl-ACP; acyl-[acyl-carrier protein]; GPAT, glycerol-3-phosphate acyltransferase; LPAT, lysophosphatidic acid acyltransferase; LPCAT, lysophosphatidylcholine acyltransferase; PAP, phosphatidic acid phosphatase; PDAT, phospholipid:diacylglycerol acyltransferase; PDCT; phosphatidylcholine:diacylglycerol cholinephosphotransferase; PLC, phospholipase C; PLD, phospholipase D; FATA, acyl-ACP thioesterase A; FATB fatty-acyl-ACP thioesterase B; SAD stearoyl-ACP desaturase; LACS long chain Acyl-CoA synthase. The figure was designed using Biorender (https://biorender.com/) under the agreements #WP24EXP3FQ and #MA24EXOUNC.

Figure. 2

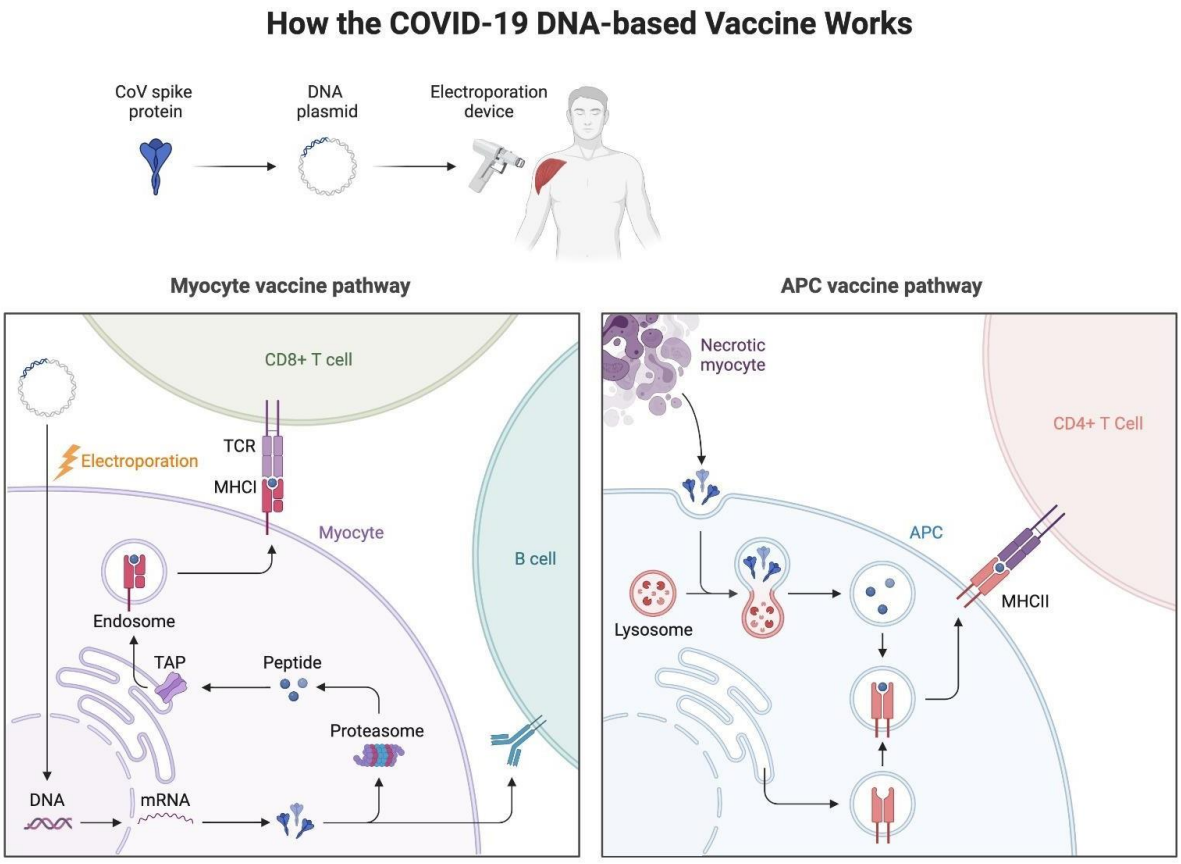
How the COVID-19 DNA-based Vaccine Works
CoV spike protein
DNA plasmid
Electroporation device
Myocyte vaccine pathway
APC vaccine pathway
CD8+ T cell
Electroporation
TCR
MHCI
Myocyte
B cell
Endosome
TAP
Peptide
Proteasome
DNA
mRNA
Necrotic myocyte
CD4+ T Cell
APC
Lysosome
MHCII

Figure. 3

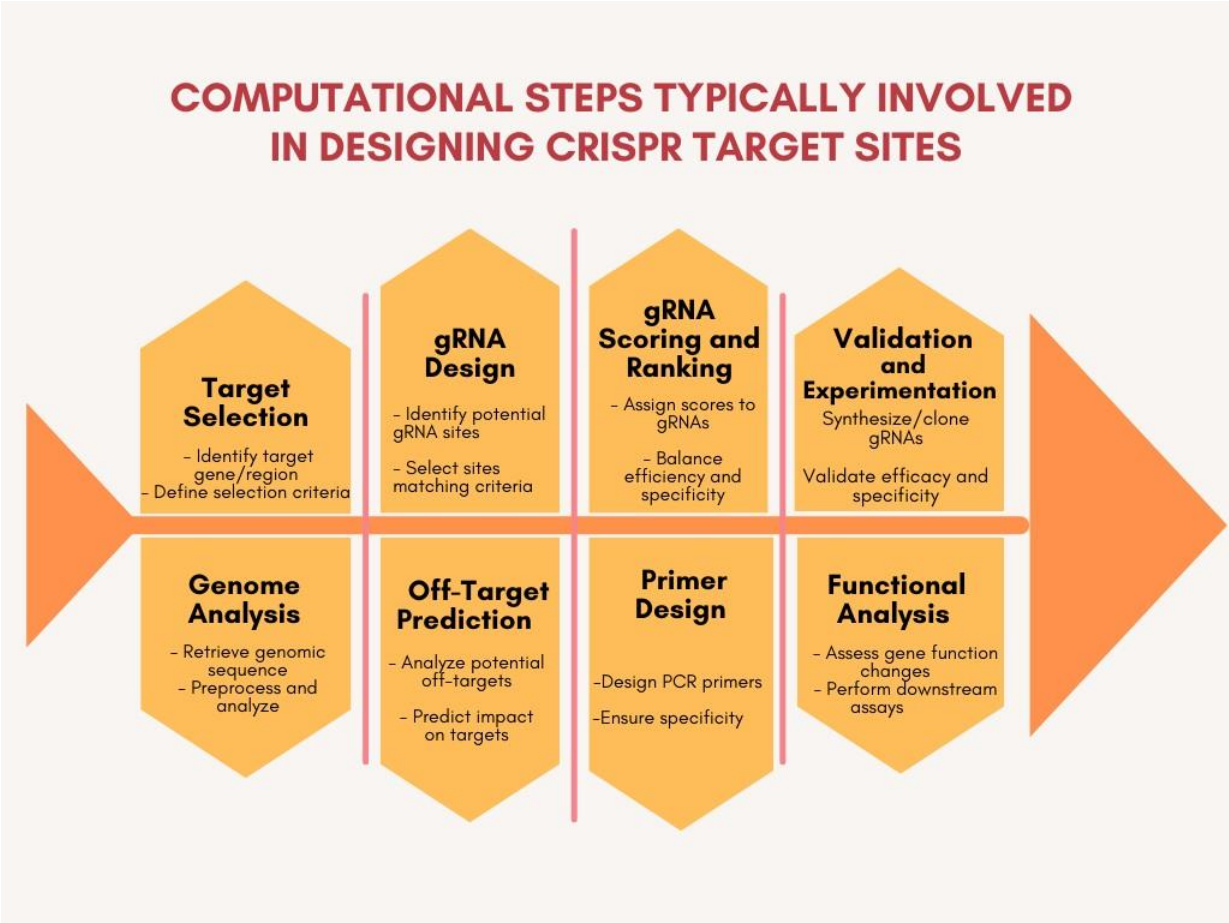
COMPUTATIONAL STEPS TYPICALLY INVOLVED IN DESIGNING CRISPR TARGET SITES
Target Selection
- Identify target gene/region
- Define selection criteria
gRNA Design
- Identify potential gRNA sites
- Select sites matching criteria
gRNA Scoring and Ranking
- Assign scores to gRNAs
- Balance efficiency and specificity
Validation and Experimentation
Synthesize/clone gRNAs
Validate efficacy and specificity
Genome Analysis
- Retrieve genomic sequence
- Preprocess and analyze
Off-Target Prediction
- Analyze potential off-targets
- Predict impact on targets
Primer Design
-Design PCR primers
-Ensure specificity
Functional Analysis
- Assess gene function changes
- Perform downstream assays

Figure. 4

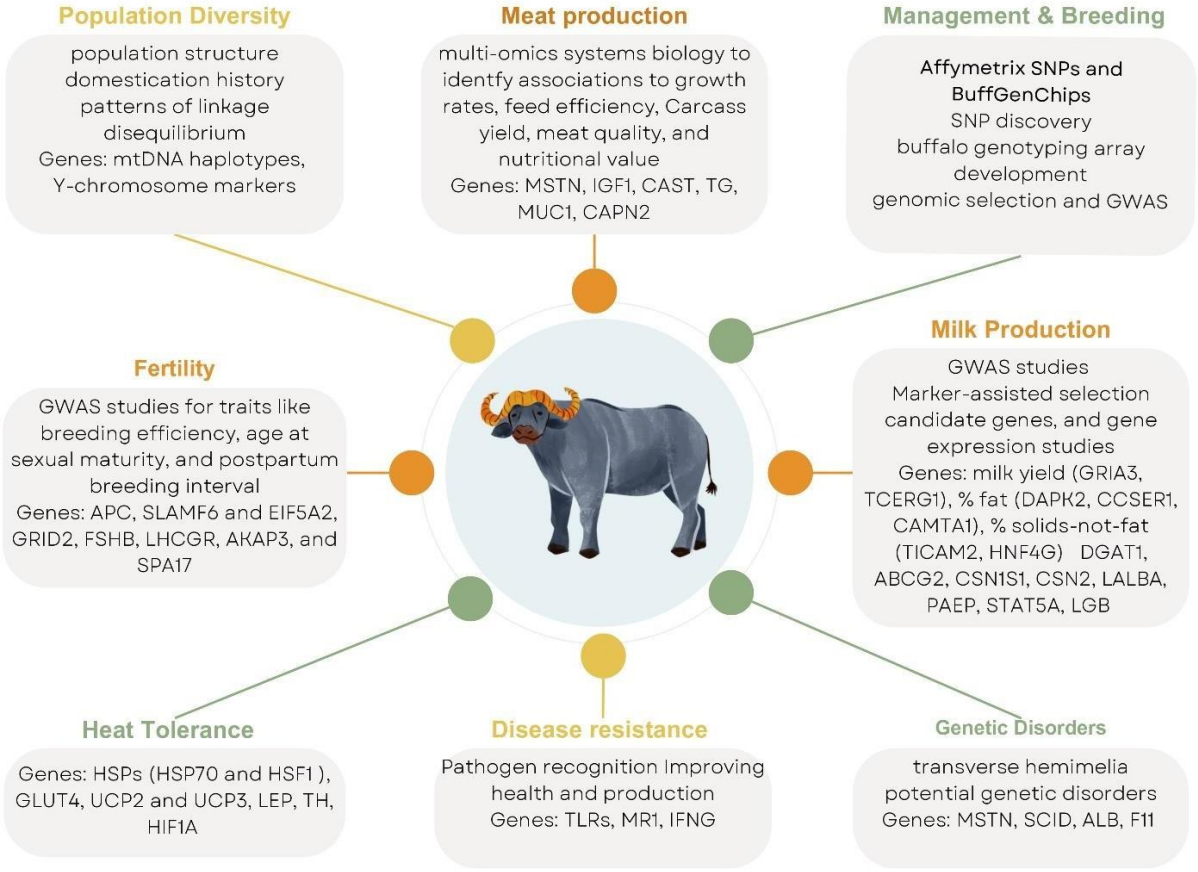
Population Diversity
population structure
domestication history
patterns of linkage disequilibrium
Genes: mtDNA haplotypes, Y-chromosome markers
Meat production
multi-omics systems biology to identfy associations to growth rates, feed efficiency, Carcass yield, meat quality, and nutritional value
Genes: MSTN, IGF1, CAST, TG, MUC1, CAPN2
Management & Breeding
Affymetrix SNPs and BuffGenChips
SNP discovery
buffalo genotyping array development
genomic selection and GWAS
Fertility
GWAS studies for traits like breeding efficiency, age at sexual maturity, and postpartum breeding interval
Genes: APC, SLAMF6 and EIF5A2, GRID2, FSHB, LHCGR, AKAP3, and SPA17
Milk Production
GWAS studies
Marker-assisted selection candidate genes, and gene expression studies
Genes: milk yield (GRIA3, TCERG1), % fat (DAPK2, CCSER1, CAMTA1), % solids-not-fat (TICAM2, HNF4G) DGAT1, ABCG2, CSN1S1, CSN2, LALBA, PAEP, STAT5A, LGB
Heat Tolerance
Genes: HSPs (HSP70 and HSF1), GLUT4, UCP2 and UCP3, LEP, TH, HIF1A
Disease resistance
Pathogen recognition Improving health and production
Genes: TLRs, MR1, IFNG
Genetic Disorders
transverse hemimelia
potential genetic disorders
Genes: MSTN, SCID, ALB, F11

Figure. 5

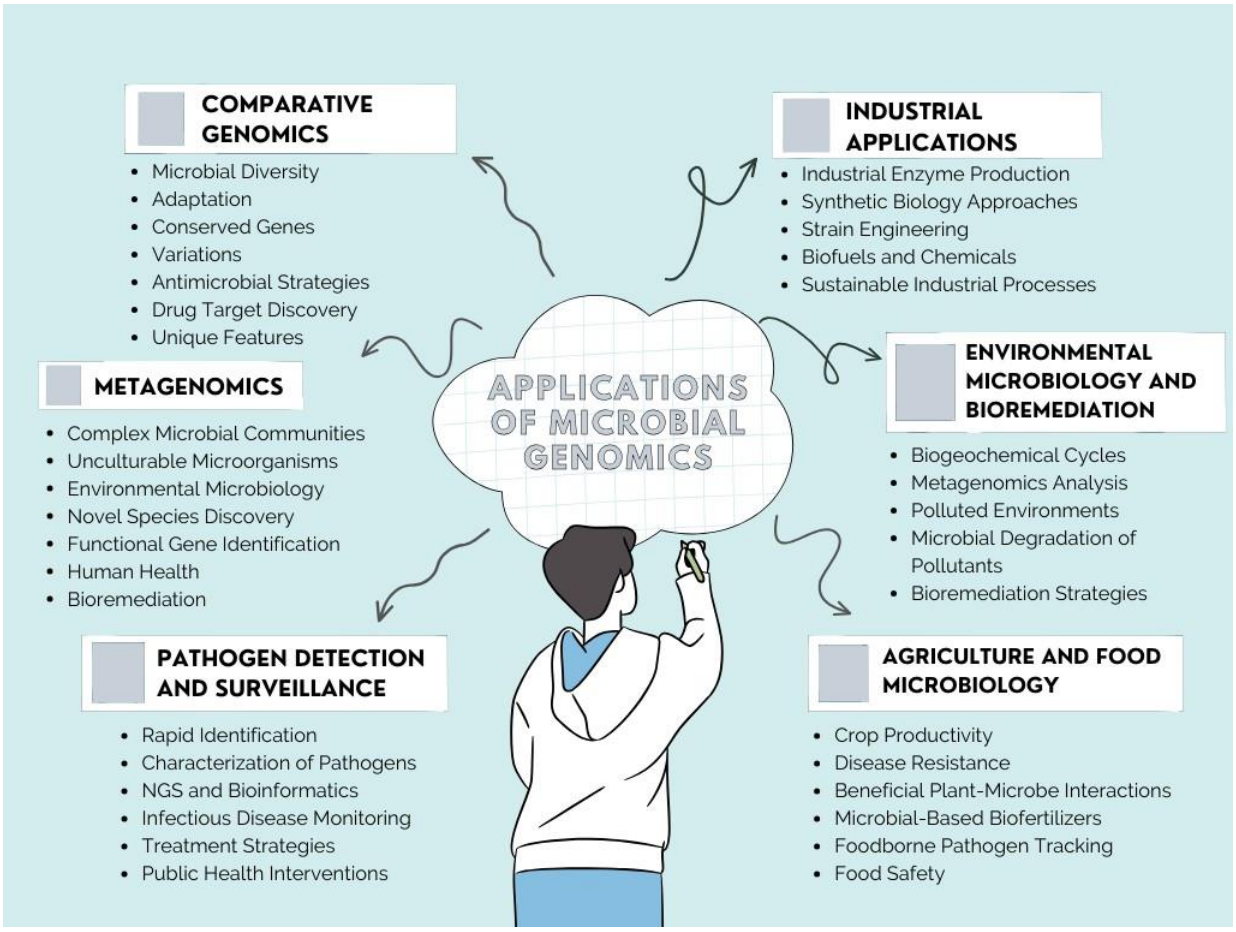
COMPARATIVE GENOMICS
Microbial Diversity
Adaptation
Conserved Genes
Variations
Antimicrobial Strategies
Drug Target Discovery
Unique Features
INDUSTRIAL APPLICATIONS
Industrial Enzyme Production
Synthetic Biology Approaches
Strain Engineering
Biofuels and Chemicals
Sustainable Industrial Processes
METAGENOMICS
Complex Microbial Communities
Unculturable Microorganisms
Environmental Microbiology
Novel Species Discovery
Functional Gene Identification
Human Health
Bioremediation
APPLICATIONS OF MICROBIAL GENOMICS
ENVIRONMENTAL MICROBIOLOGY AND BIOREMEDIATION
Biogeochemical Cycles
Metagenomics Analysis
Polluted Environments
Microbial Degradation of Pollutants
Bioremediation Strategies
PATHOGEN DETECTION AND SURVEILLANCE
Rapid Identification
Characterization of Pathogens
NGS and Bioinformatics
Infectious Disease Monitoring
Treatment Strategies
Public Health Interventions
AGRICULTURE AND FOOD MICROBIOLOGY
Crop Productivity
Disease Resistance
Beneficial Plant-Microbe Interactions
Microbial-Based Biofertilizers
Foodborne Pathogen Tracking
Food Safety

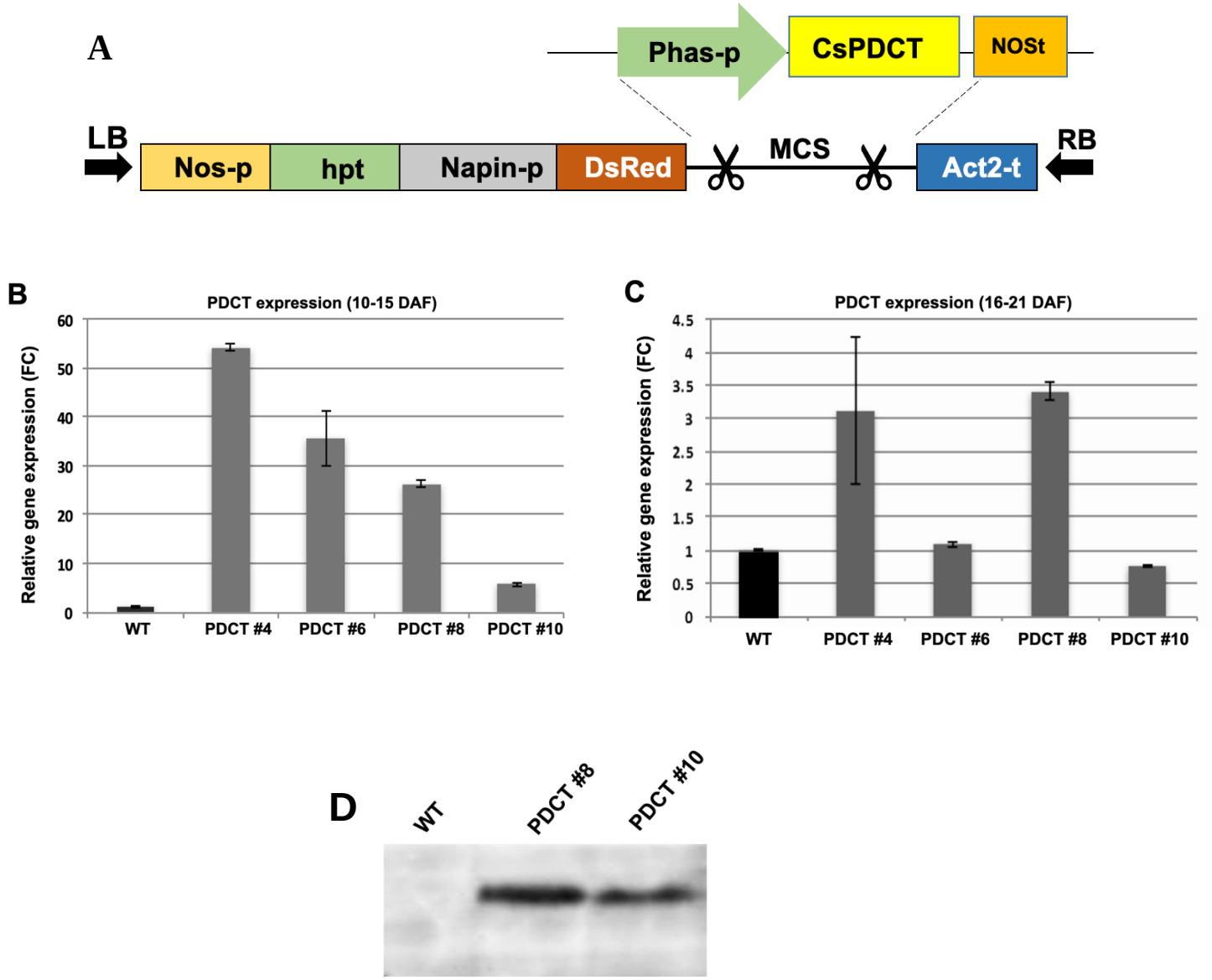

Figure. 6 The T-DNA insertion used to transform *Camelina sativa* and the gene expression confirmation of PDCT using qRT-PCR. **(A)** the modified pCambia RedSeed binary vector containing seed-specific cassettes for expression of the Camelina PDCT under the control of seed-specific beta-type Phaseolin promoter from *Phaselous vulgaris*. DsRed fluorescence marker and the hygromycin-resistant *hpt* gene for selection of transformants are shown in the phas::PDCT construct. **(B and C)** the analysis of PDCT transcript expression in Camelina developing seeds of T3 generation homozygous transgenic lines overexpressing PDCT and in their parental non-transgenic WT in 10-15 and 16-21 DAF, respectively. **(D)** Immunoblot using 1:500 dilution of HA-tag primary antibody and 1:10000 dilution of Licor Goat anti mouse secondary antibody 800cw in each well on the 12% SDS-PAGE gels, ~ 50ug of total protein was loaded in SDS gel as determined by the Dot plot Assay. A PVDF membrane was used for the transfer and this image was exposed using Licor at 800cw. CsPDCT is ~ 32 kDa. Proteins were extracted from 14 days after flowering (DAF) seeds. Values in (B and C) are the means of fold change ± standard error SE estimated from three independent qRT-PCR measurements. Gene expression levels were normalized with respect to the internal control *Actin2* gene. The value in WT samples were always adjusted to 1 as they are calibrators for normalizing relative gene expression. DAF, days after flowering; Nos-p, nopaline synthase promoter; Napin-p, napin promoter from *Brassica napus*; MCS, multiple cloning site; Nos-t, nopaline synthase terminator; Act2-t, Actin 2 terminator.

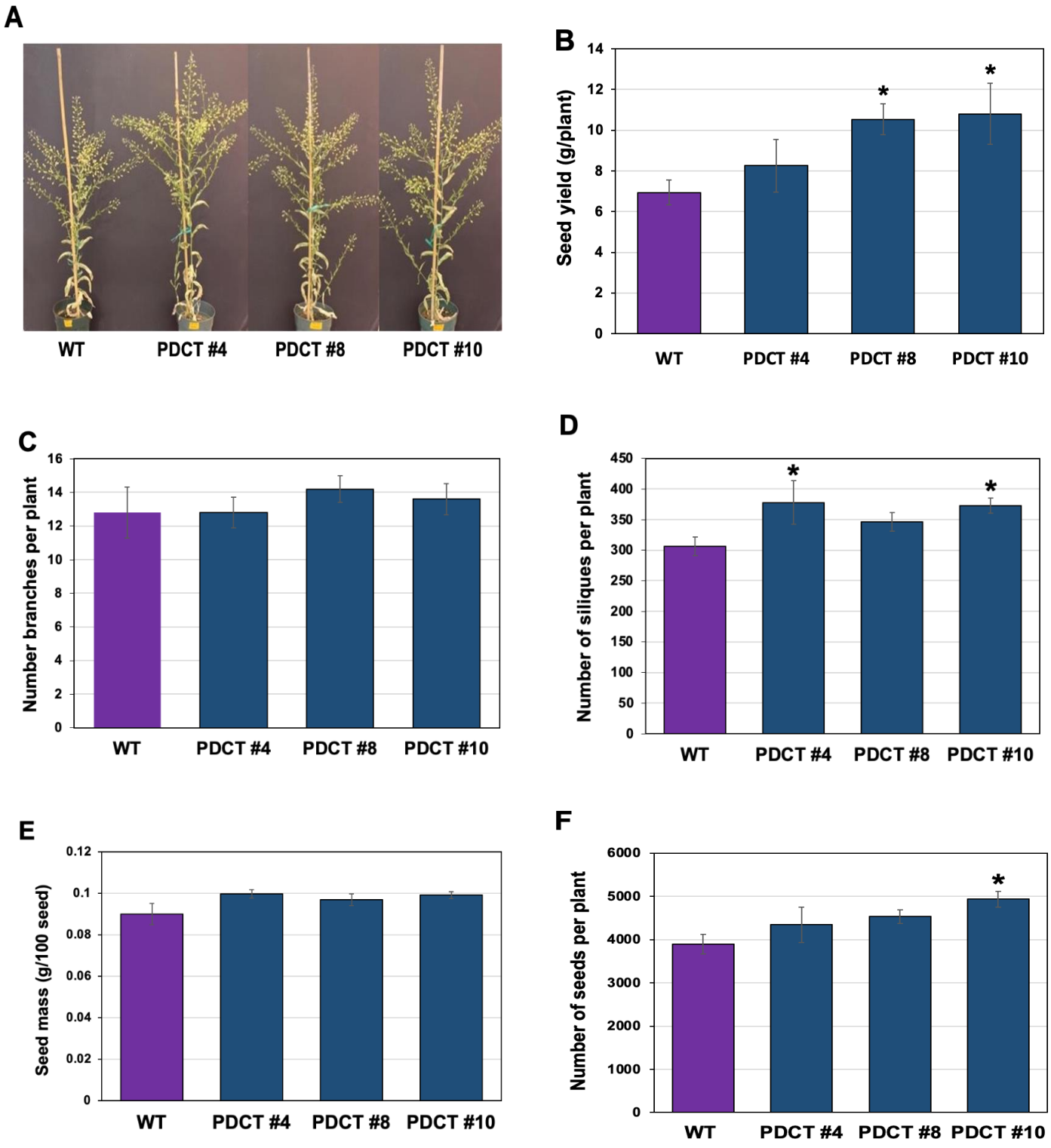

Figure.7 Effect of PDCT overexpression on Camelina morphological characteristics and seeds attributes. The morphology of the 8-weeks old plants (**A**), average seed yield (**B**), average number of branches (**C**), average number of siliques/pods (**D**), average seed size (**E**), average number of seeds (**F**) are shown. Data are means ± standard error (SE) on measurements on homozygous T4 seeds from individual plants (*n*= 6-8) of each genotype grown under controlled growth conditions. Asterisks denote significance of differences between WT and PDCT transgenic lines (Dunnett test *P < 0.05).

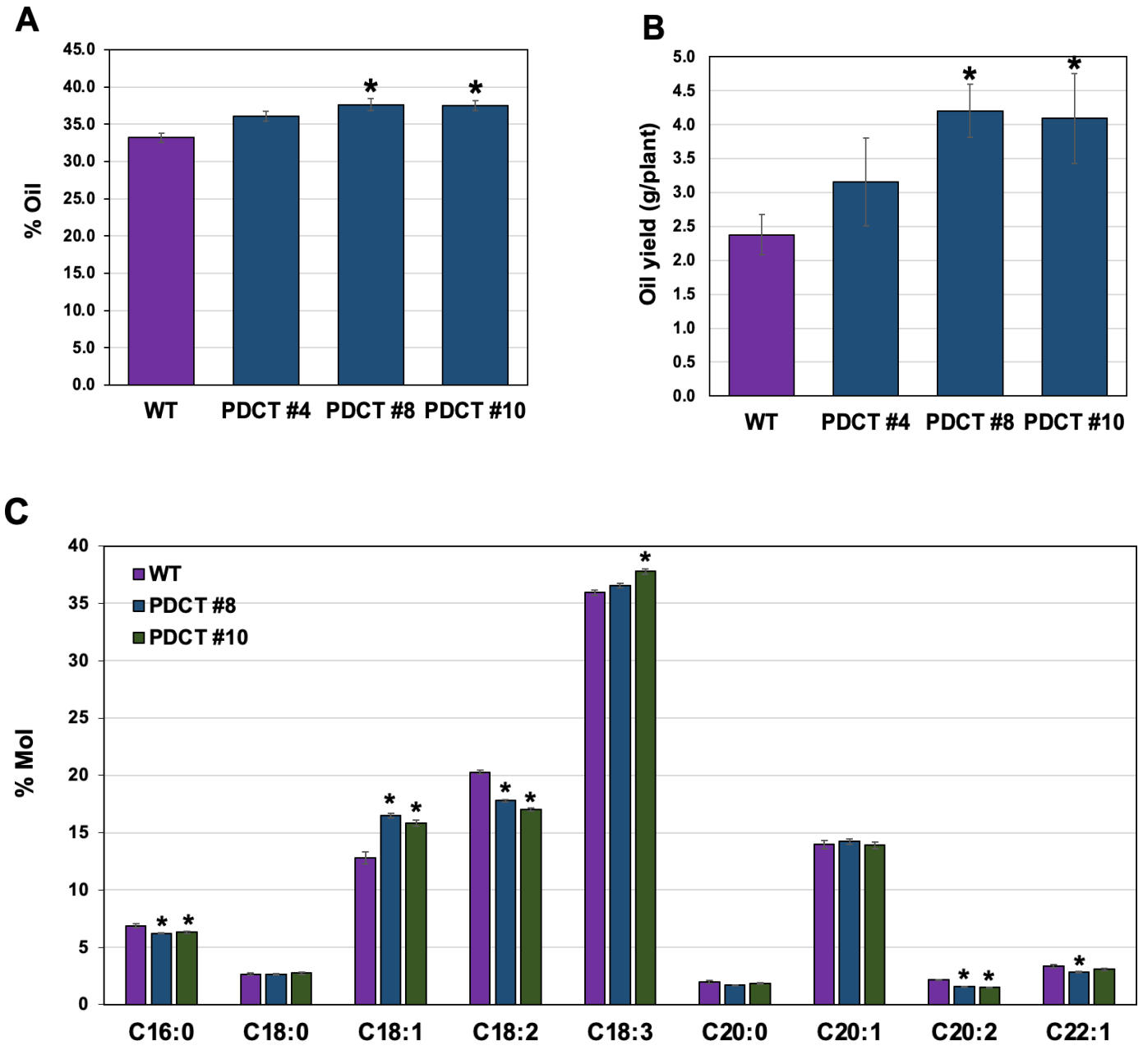

Figure. 8 Effect of PDCT overexpression on Camelina seed oil attributes. % oil content (**A**), oil yield (**B**), and FAME composition (**C**) of WT and T4 transgenic homozygous seeds from individual plants (*n*= 6-8) of each genotype grown under controlled growth conditions, relative to their parental WT plants. The data from selected elite lines expressing PDCT gene are shown. Asterisks denote significance of differences between WT and PDCT transgenic lines (Dunnett test *P < 0.05).

A

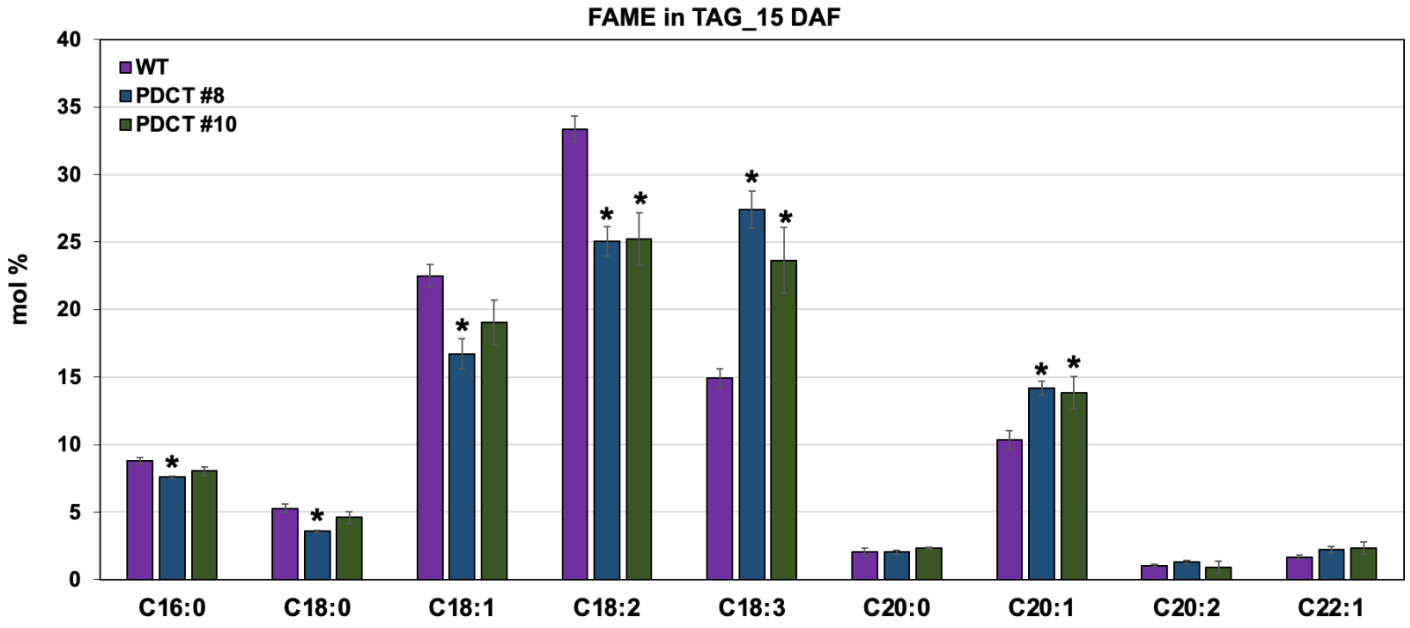
FAME in TAG_15 DAF
WT
PDCT #8
PDCT #10
mol %
40
35
30
25
20
15
10
5
0
C16:0
C18:0
C18:1
C18:2
C18:3
C20:0
C20:1
C20:2
C22:1

B

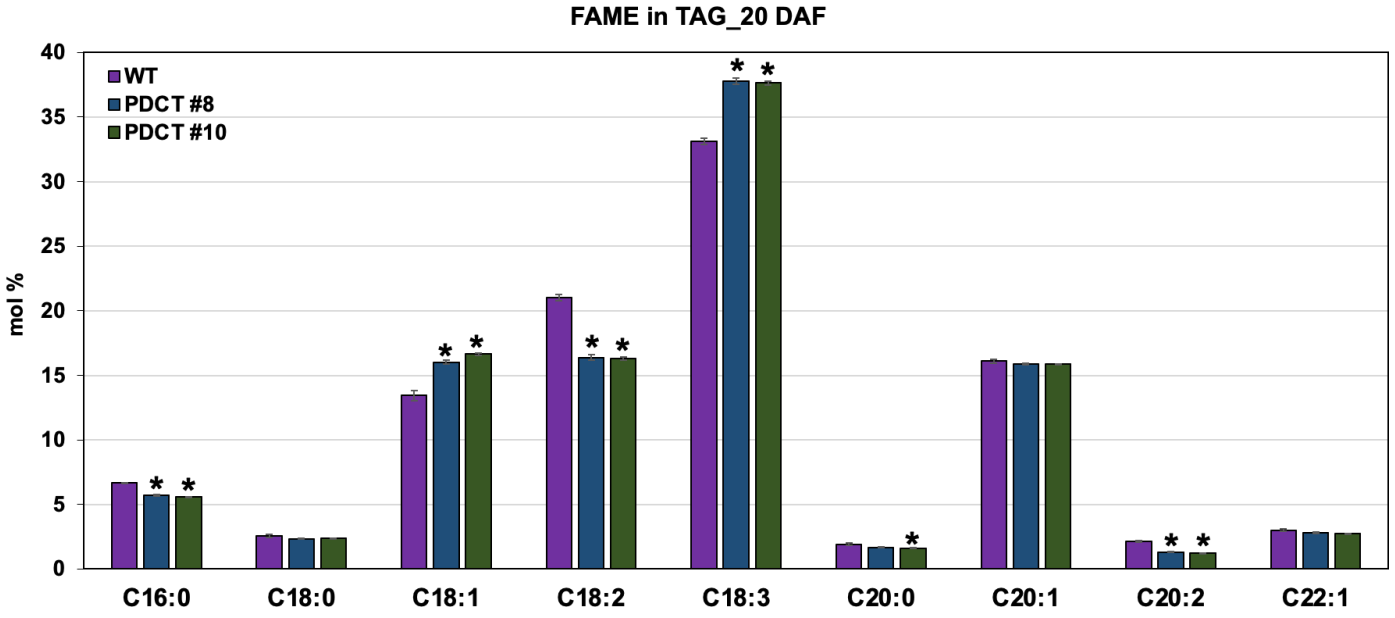
FAME in TAG_20 DAF
WT
PDCT #8
PDCT #10
mol %
40
35
30
25
20
15
10
5
0
C16:0
C18:0
C18:1
C18:2
C18:3
C20:0
C20:1
C20:2
C22:1

C

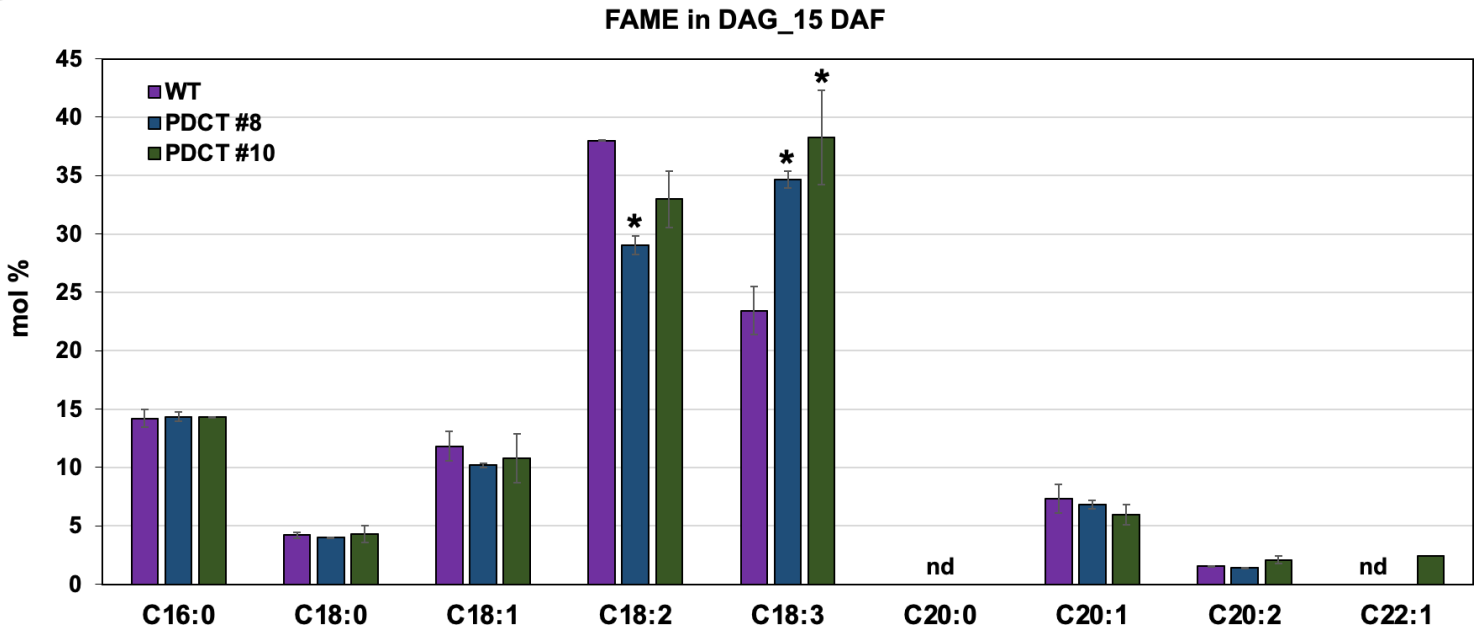
FAME in DAG_15 DAF
WT
PDCT #8
PDCT #10
mol %
45
40
35
30
25
20
15
10
5
0
*
*
*
nd
nd
C16:0
C18:0
C18:1
C18:2
C18:3
C20:0
C20:1
C20:2
C22:1

D

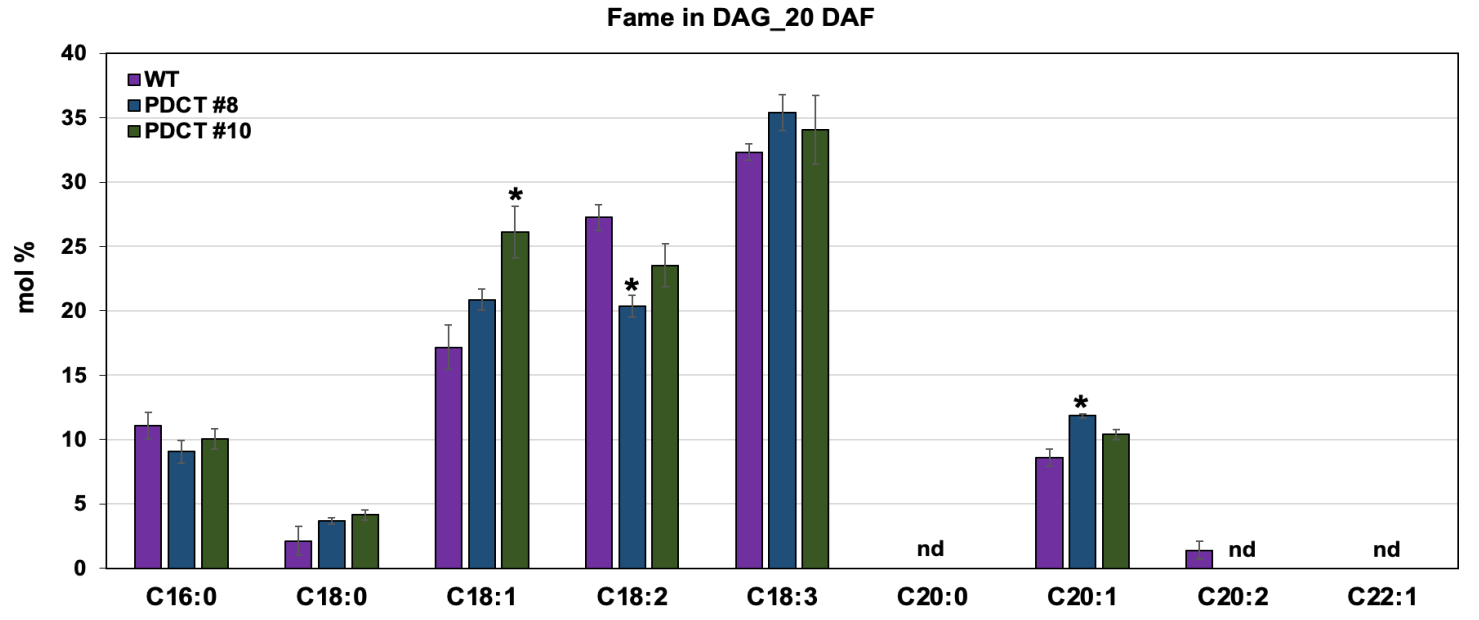
Fame in DAG_20 DAF
WT
PDCT #8
PDCT #10
mol %
40
35
30
25
20
15
10
5
0
*
*
*
nd
nd
nd
C16:0
C18:0
C18:1
C18:2
C18:3
C20:0
C20:1
C20:2
C22:1

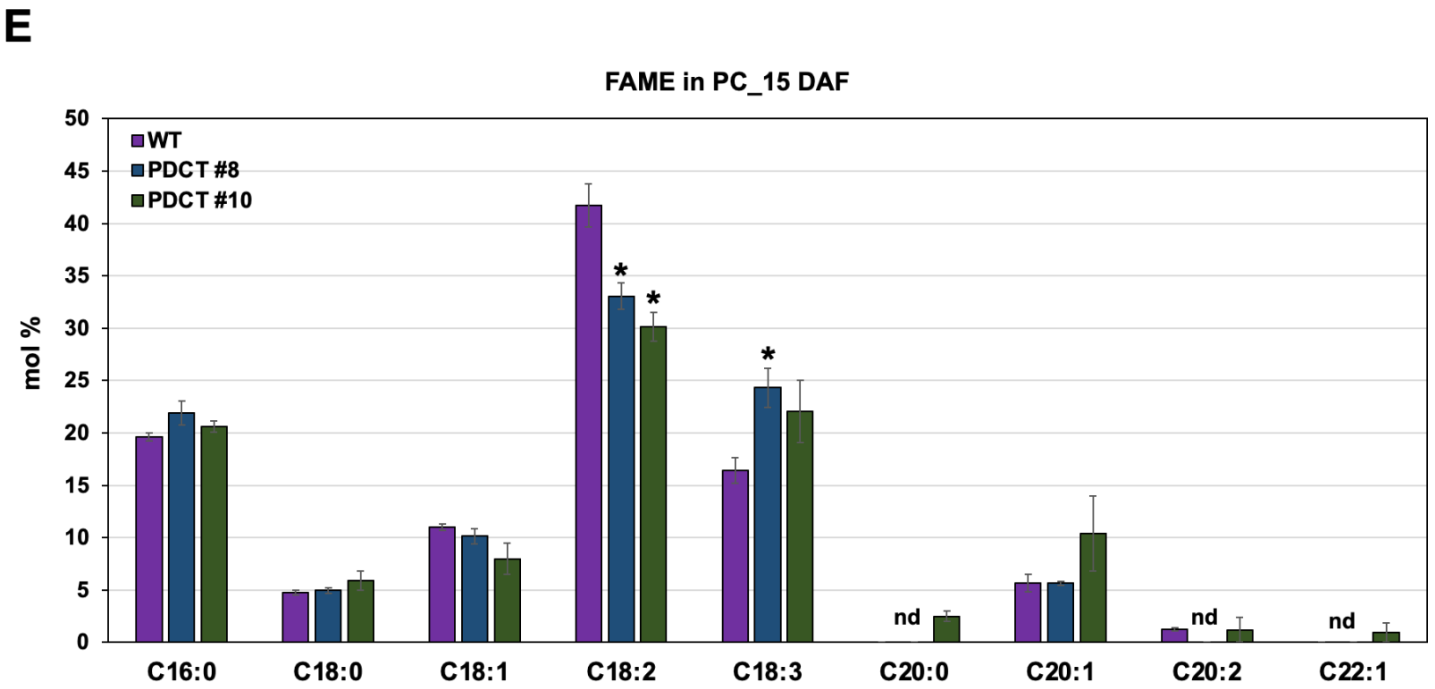

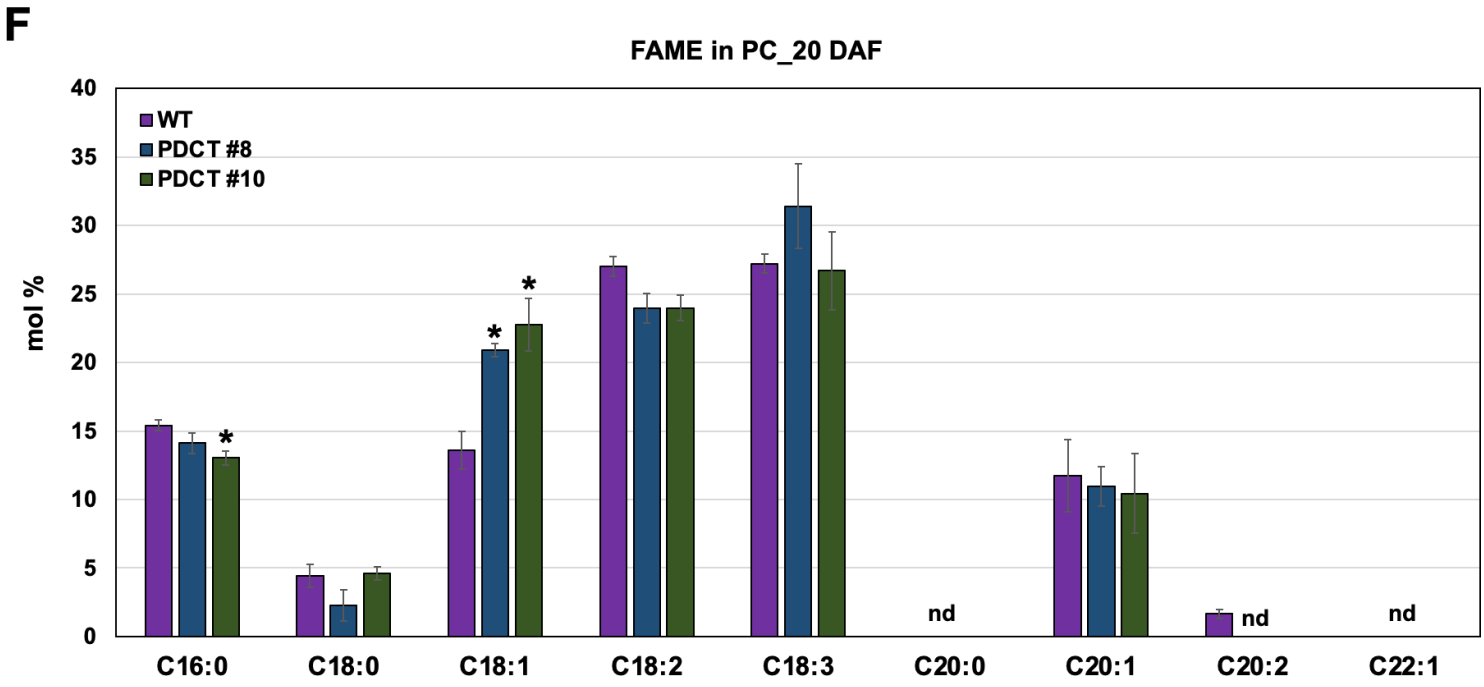

Figure. 9 Fatty acid compositions of TAG, DAG, and PC extracted from developing seeds of WT and PDCT expressing lines. Seeds were harvested 15 and 20 days after flowering (DAF), the periods at which the oil synthesis rate is maximum. Shown are FAME compositions of common fatty acids in WT and T3 transgenic homozygous seeds from three independent biological replicates (n= 3) of each genotype grown under controlled growth conditions. The data in (A) and (B) are FAME in TAG at 15 and 20 DAF, respectively. The data in (C) and (D) are FAME in DAG at 15 and 20 DAF, respectively. The data in (E) and (F) are FAME in PC at 15 and 20 DAF, respectively. The data from selected elite lines expressing the PDCT gene and WT are shown. Asterisks denote significance of differences between WT and PDCT transgenic lines (Dunnett test *P < 0.05). TAG: triacylglycerol, DAG: diacylglycerol, PC: phosphatidylcholine. nd, not detected.

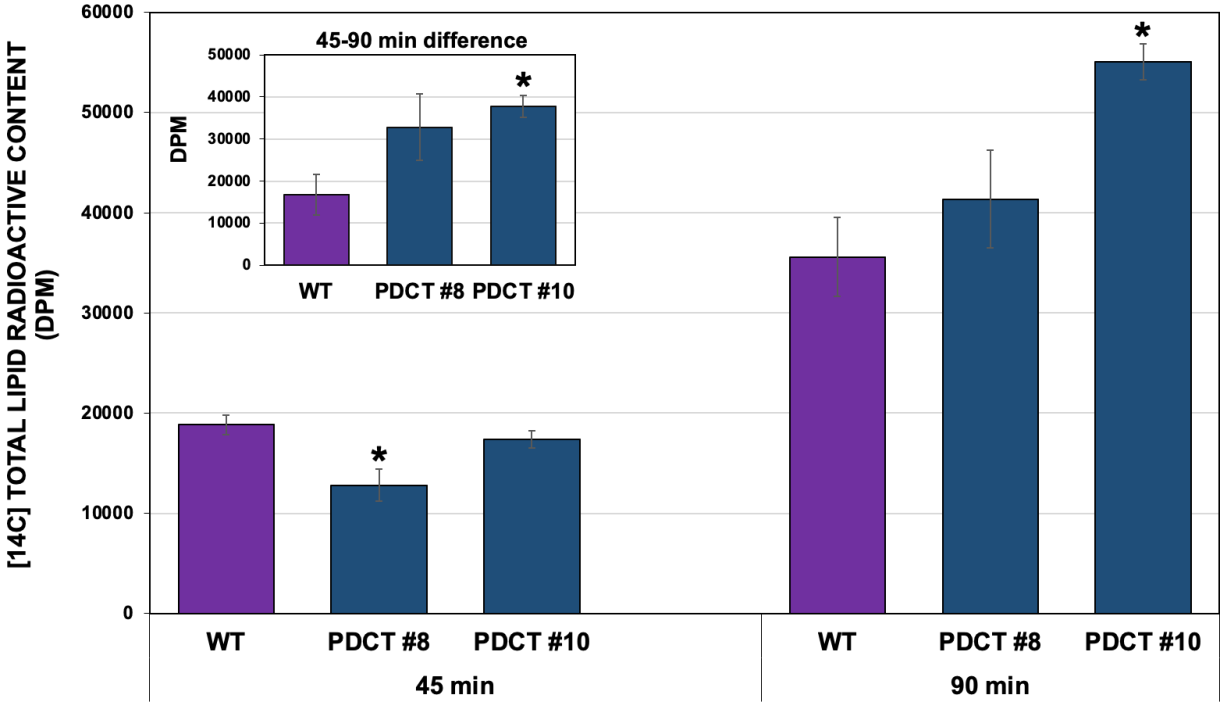

Figure. 10 Radioactivity [disintegrations per minute (DPM)] of the radiolabeled total lipids in Camelina embryos 15 DAF at 45 and 90 min of incubation with [14C]acetate. WT and two elite PDCT expressing lines are shown. The flux change rates are shown. Data is disintegrations per minute DPM/embryo. Asterisks denote significance of differences between WT and PDCT transgenic lines (Dunnett test *P < 0.05).

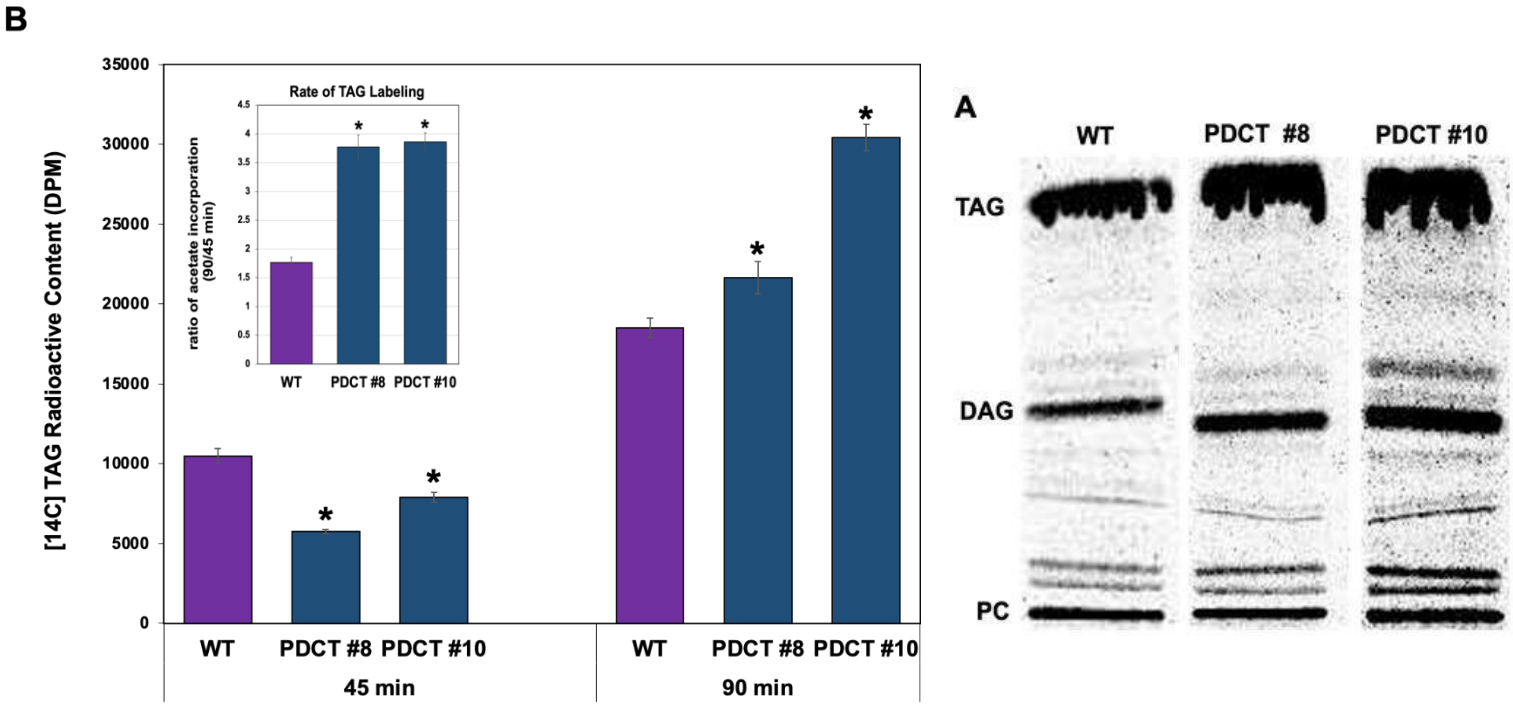

Figure. 11 TLC analyses and phosphoimaging quantification of [^{14}C]lipids in Camelina embryos. Panel **A** shows TLC separation of neutral and polar lipids in 15 DAF embryos at 90 min of incubation with [^{14}C]acetate. WT and two elite PDCT expressing lines are shown. Panel **B** shows the quantification of radioactive content in TAG lipids in PDCT embryos relative WT embryos cultured with [^{14}C]acetate for 45 and 90 minutes. The small panel indicates the rate of change of [^{14}C]acetate content between 45 and 90 min of culturing with [^{14}C]acetate in TAG. Data is disintegrations per minute DPM/embryo. TAG: triacylglycerol, DAG: diacylglycerol, PC: phosphatidylcholine. Asterisks denote significance of differences between WT and PDCT transgenic lines (Dunnett test *P < 0.05).

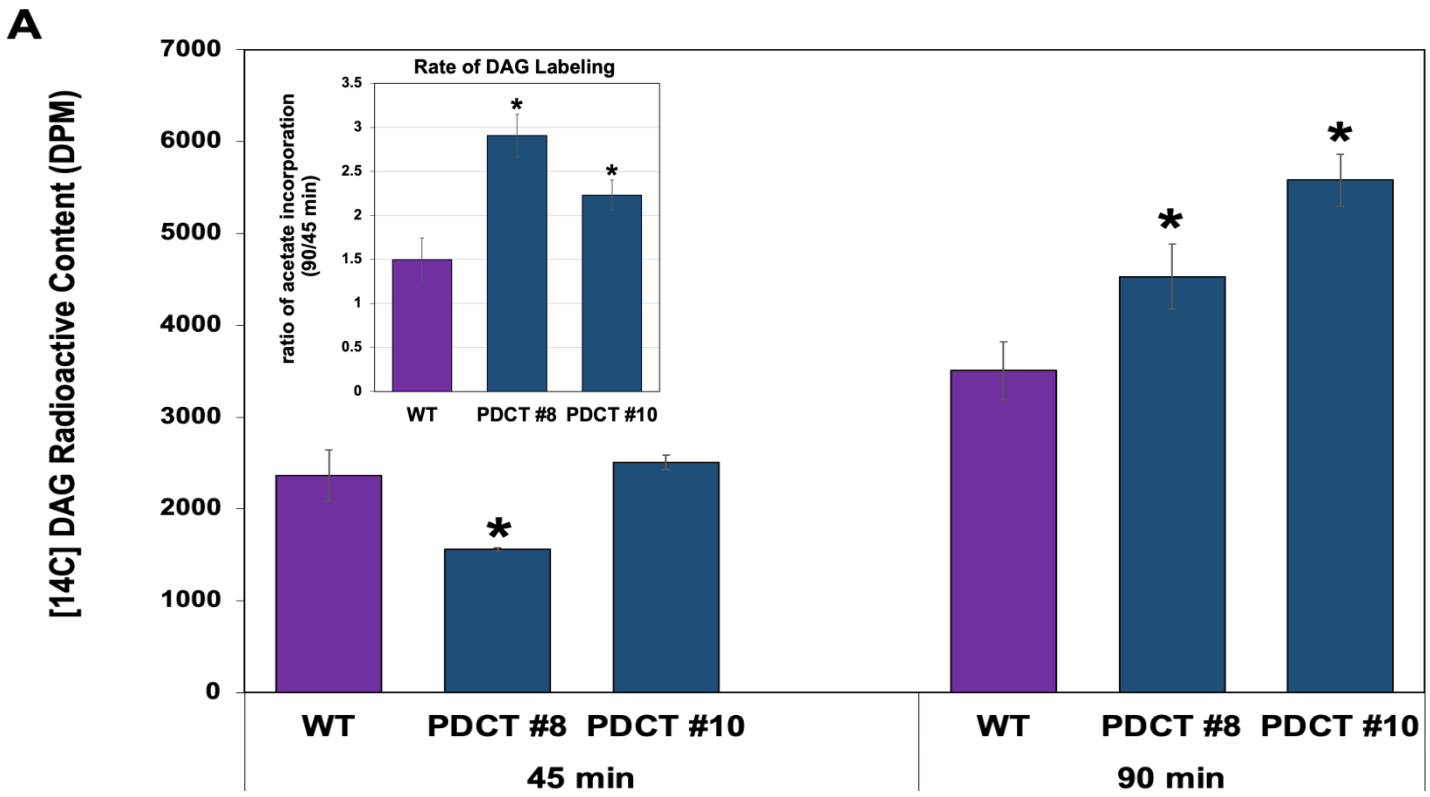
A
[14C] DAG Radioactive Content (DPM)
7000
6000
5000
4000
3000
2000
1000
0
Rate of DAG Labeling
ratio of acetate incorporation (90/45 min)
3.5
3
2.5
2
1.5
1
0.5
0
*
*
WT
PDCT #8
PDCT #10
*
*
WT
PDCT #8
PDCT #10
45 min
WT
PDCT #8
PDCT #10
90 min

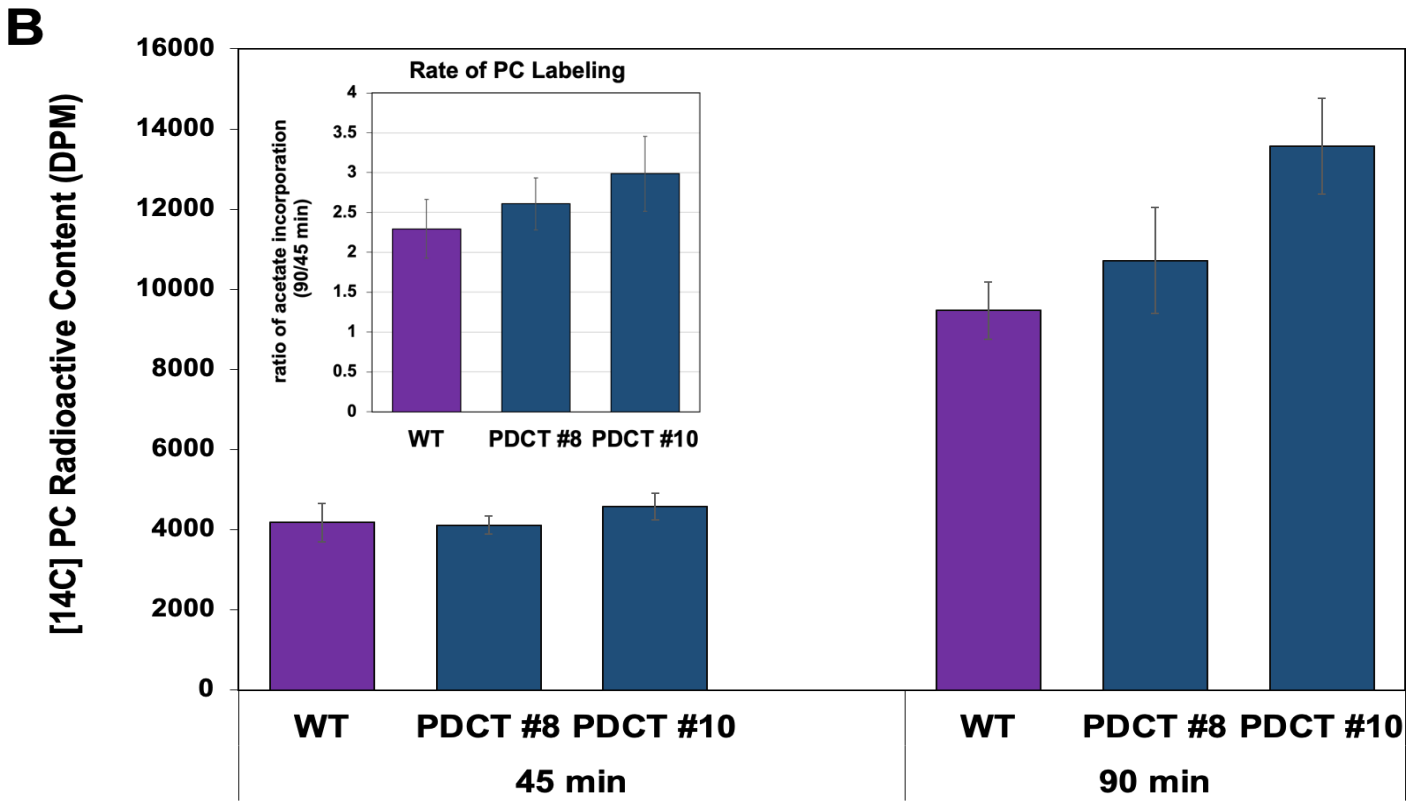
B
[14C] PC Radioactive Content (DPM)
16000
14000
12000
10000
8000
6000
4000
2000
0
Rate of PC Labeling
ratio of acetate incorporation (90/45 min)
4
3.5
3
2.5
2
1.5
1
0.5
0
WT
PDCT #8
PDCT #10
WT
PDCT #8
PDCT #10
45 min
WT
PDCT #8
PDCT #10
90 min

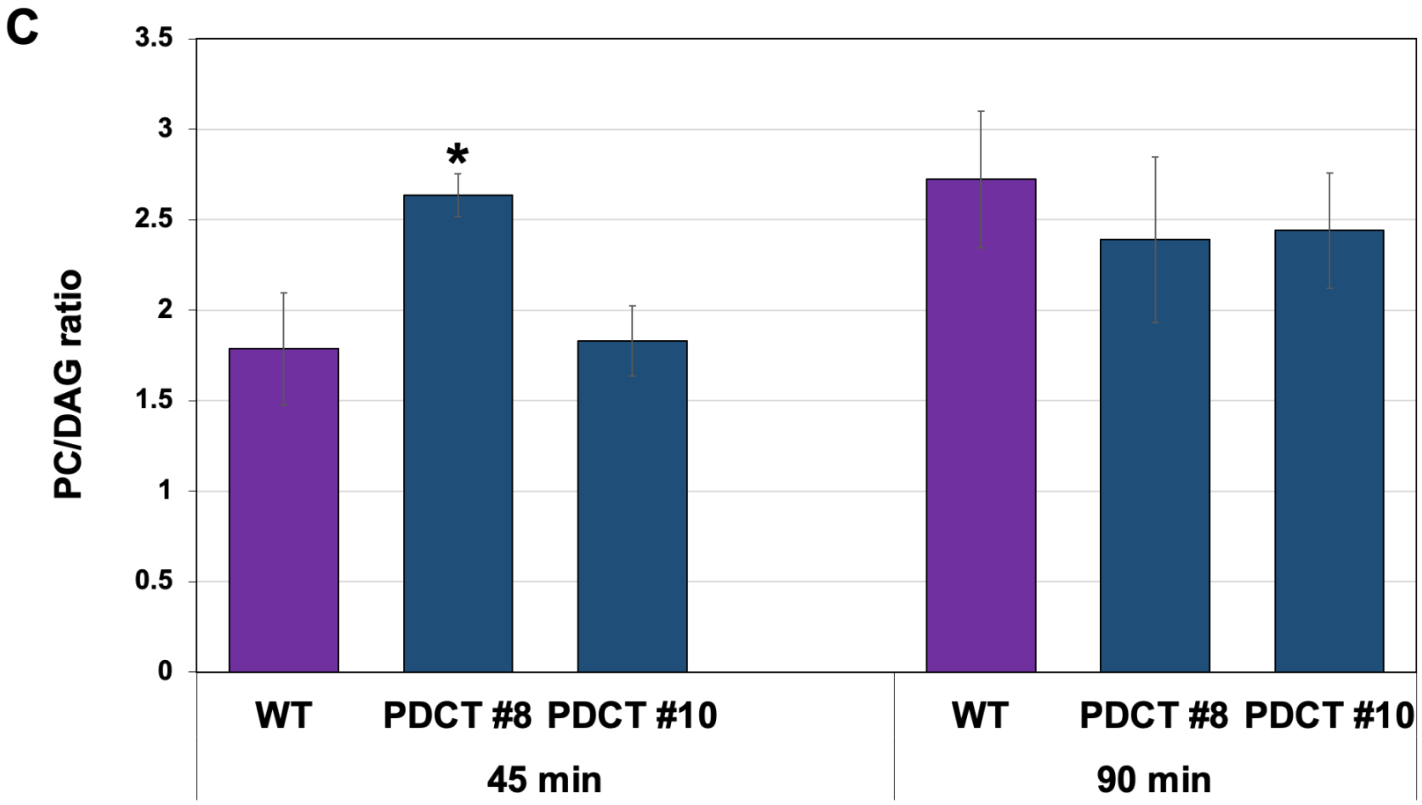

Figure. 12 Phosphoimaging quantification of [^{14}C]lipids in Camelina embryos. Panels **A** and **B** show the quantification of radioactive content in DAG and PC lipids, respectively, in PDCT embryos relative WT embryos cultured with [^{14}C]acetate for 45 and 90 minutes. The small panel in **A** and **B** indicates the rate of change of [^{14}C]acetate content between 45 and 90 min of culturing with [^{14}C]acetate in DAG and PC, respectively. Panel **C** shows the ratio of relative PC content to the relative of DAG content in WT and transgenic PDCT embryos. WT and two elite PDCT expressing lines are shown. Data is disintegrations per minute DPM/embryo. TAG: triacylglycerol, DAG: diacylglycerol, PC: phosphatidylcholine. Asterisks denote significance of differences between WT and PDCT transgenic lines (Dunnett test *P < 0.05).